Sunspot, a link between Wingless signaling and endoreplication in *Drosophila*

Kenzui Taniue[1],*, Ayumu Nishida[1],*, Fumihiko Hamada[2], Atsushi Sugie[3], Takeaki Oda[1], Kumiko Ui-Tei[4], Tetsuya Tabata[3] and Tetsu Akiyama[1],†

SUMMARY

The Wingless (Wg)/Wnt signaling pathway is highly conserved throughout many multicellular organisms. It directs the development of diverse tissues and organs by regulating important processes such as proliferation, polarity and the specification of cell fates. Upon activation of the Wg/Wnt signaling pathway, Armadillo (Arm)/β-catenin is stabilized and interacts with the TCF family of transcription factors, which in turn activate Wnt target genes. We show here that Arm interacts with a novel BED (BEAF and Dref) finger protein that we have termed Sunspot (Ssp). Ssp transactivates *Drosophila E2F-1* (*dE2F-1*) and *PCNA* expression, and positively regulates the proliferation of imaginal disc cells and the endoreplication of salivary gland cells. Wg negatively regulates the function of Ssp by changing its subcellular localization in the salivary gland. In addition, Ssp was found not to be involved in the signaling pathway mediated by Arm associated with dTCF. Our findings indicate that Arm controls development in part by regulating the function of Ssp.

KEY WORDS: Sunspot, Armadillo, Wingless, E2F, BED finger, Endoreplication, *Drosophila*

INTRODUCTION

The Wnt/Wingless (Wg) signaling transduction pathway controls cell fate, asymmetric cell division and stem cell behavior, and thereby regulates many developmental processes (Cadigan and Nusse, 1997; Moon et al., 2004; Clevers, 2006). Wnt/Wg signaling is also involved in tumorigenesis. For example, mutations of the Wnt regulator adenomatous polyposis coli (APC) are responsible for colorectal tumorigenesis (Peifer and Polakis, 2000; Fodde et al., 2001; Bienz, 2002; Segditsas and Tomlinson, 2006).

The Wnt family of proteins consists of more than 20 closely related secreted glycoproteins. Receptors for the Wnt proteins are members of the Frizzled family of transmembrane proteins, and the Wnt signal is transduced to the cytoplasm. Upon activation by the Wnt signal, β-catenin/Armadillo (Arm) is stabilized, resulting in its accumulation and consequent formation of a complex with the TCF/LEF family of transcription factors. The β-catenin–TCF complex in turn activates the transcription of downstream genes, such as *c-Myc* and *Axin2*. In the absence of Wnt signaling, β-catenin is targeted for proteasome-mediated degradation by the multi-protein complex containing APC, glycogen synthase kinase 3β (GSK3β), casein kinase 1α and Axin or the closely related factor Axin2/conductin/axil. Whereas intact APC normally induces the degradation of β-catenin, mutant APCs found in most colon cancers are defective in this activity (Kinzler and Vogelstein, 1996; Nagase and Nakamura, 1993). In addition, in a small percentage of colon tumours, β-catenin is mutated and is resistant to APC-mediated degradation (Fodde et al., 2001; Morin et al., 1997; Rubinfeld et al., 1997). Thus, the regulation of β-catenin stability and, consequently, of β-catenin–TCF/LEF-mediated transactivation are crucial for Wnt signaling during development and tumorigenesis.

In the present study, we show that β-catenin/Arm interacts with a novel protein, Sunspot (Ssp), and that Ssp plays an important role in the regulation of endoreplication in the salivary gland of *Drosophila*. Furthermore, we demonstrate that Wg represses the function of Ssp by altering the subcellular localization of Ssp, and thereby negatively regulates endoreplication.

MATERIALS AND METHODS

Fly stocks

UAS-ssp, *UAS-GFP-ssp* and *UAS-GFP-sspΔC* lines were generated by *P*-element-mediated transformation. The following alleles are a P *lacZ* enhancer-trap insertion: *dfz3^J29^* (K. Saigo, University of Tokyo, Tokyo, Japan), *E2F^07172^* and *PCNA^02448^*. Mutant alleles, *Gal4* lines and *UAS* lines used were: *ssp^598^*, *wg^I-12^*, *Df(3L)BK9*, *arm-Gal4*, *dpp-Gal4*, *hs-Gal4*, *act>CD2>Gal4*, *UAS-wg*, *UAS-Axin*, *UAS-Δarm*, *UAS-EGFP* and *UAS-dsRNA* (*arm*; 11579R-2), which was obtained from the NIG stock center. *wg^I-12^* animals were maintained at the permissive temperature of 16°C and were shifted to a nonpermissive temperature of 29°C for 72 hours prior to analysis. *UAS-Δarm* expresses a mutant of Arm that lacks the N-terminal 128 amino acids and that has an N-terminal HA tag and a consensus myristoylation site (Zecca et al., 1996). For flip-out clones, clones were induced for 72-96 hours prior to analysis.

Antibodies

Polyclonal antibody (pAb) to Ssp was prepared by immunizing rabbits with peptide containing amino acids 235-307 of Ssp. The antibody was purified by affinity chromatography using columns to which the antigens used for immunization had been linked.

Two-hybrid system

The target was generated by fusing the Armadillo repeats of Arm (amino acids 140 to 713) to the DNA-binding domain of yeast GAL4 in the vector pGBT9. We screened 6×10^6 clones of a *Drosophila* embryo cDNA library (Clontech) fused to the transcription activation domain of yeast GAL4 in the

[1]Laboratory of Molecular and Genetic Information, Institute of Molecular and Cellular Biosciences, University of Tokyo, Tokyo 113-0032, Japan. [2]Department of Human Anatomy, Oita University Faculty of Medicine, Oita 879-5593, Japan. [3]Laboratory of Morphogenesis, Institute of Molecular and Cellular Biosciences, University of Tokyo, Tokyo 113-0032, Japan. [4]Department of Biophysics and Biochemistry, Graduate School of Science, University of Tokyo, Tokyo 113-0032, Japan.

*These authors contributed equally to this work
†Author for correspondence (akiyama@iam.u-tokyo.ac.jp)

vector pGAD10 and isolated a fragment of the *ssp* cDNA. A larger partial *ssp* cDNA clone (1.5 kb) was isolated by re-screening a λgt11 *Drosophila* embryo cDNA library with the *ssp* cDNA fragment, and the remaining 5′-end region was obtained by the 5′ RACE (rapid amplification of cDNA ends) technique (Clontech).

In vitro binding assays

Full-length Ssp and the Armadillo repeat domain of Arm were labeled with biotin or ^{35}S-methionine using the coupled transcription-translation TNT system (Promega). GST and GST-fusion proteins (2 μg) immobilized to glutathione-Sepharose beads were mixed with in vitro translated proteins in binding buffer [20 mM Tris-HCl (pH 8.0), 140 mM NaCl, 1 mM EDTA, 1 mM dithiothreitol, 10% glycerol, 1% Triton X-100, and 10 mg/μl each of aprotinin, leupeptin and pepstatin] for 1 hour at 4°C. After washing five times with binding buffer, bound proteins were fractionated by SDS-polyacrylamide gel electrophoresis (PAGE) then subjected to autoradiography or immunoblotting. Immunoblotting was done by standard techniques using streptavidin-alkaline phosphatase (1:5000 dilution; Promega).

Cell culture and transfections

Drosophila Schneider-2 cells (S2) cells were cultured in Schneider's medium (Gibco) supplemented with 10% fetal bovine serum. Transient transfections were carried out in 24-well petri dishes on 0.8×10^6 S2 cells using 40 μl 250 mM CaCl$_2$, 40 μl 2×HEBS (280 mM NaCl, 10 mM KCl, 2 mM Na$_2$HPO$_4$, 12 mM dextrose, 50 mM HEPES, pH 7.1), 1.5 μg of *pACT-arm* and/or plasmid DNAs in the *pACT-GFP* backbone, such as *pACT-GFPssp*, *pACT-GFPsspΔC* and *pACT-GFPsspABR*.

Immunoprecipitation

Approximately 3×10^6 cells were used for each immunoprecipitation experiment. Cells were harvested by centrifugation 48 hours after transfection, and the pellet washed once with phosphate buffered saline (PBS). They were solubilized in 100 μl lysis buffer [10 mM Tris-HCl (pH 7.5), 150 mM NaCl, 0.5% NP-40, 0.5 mM EDTA and protease inhibitors cocktail] for 30 minutes on ice. After clarifying the cell extract by centrifugation, the volume of the supernatant was adjusted with dilution buffer [10 mM Tris-HCl (pH 7.5), 150 mM NaCl, 0.5 mM EDTA] to 400 μl and then incubated with GFP-Trap-M (10 μl; ChromoTek) (Rothbauer et al., 2008). The precipitates were washed three times with dilution buffer before loading onto a 10% SDS-polyacrylamide gel for western blotting, following standard procedures.

Immunohistochemistry

Wing imaginal discs and salivary glands from the third instar larvae were dissected, and the fat body removed, before fixing and staining with appropriate antibodies. Primary antibodies were mouse monoclonal antibody (mAb) against β-galactosidase [β-gal; 1:100; 40-1a, Developmental Studies Hybridoma Bank (DSHB)], Arm (1:100; N2 7A1, DSHB), Wg (1:1000; 4D4, DSHB), HA (1:500; 16B12, Covance), dMyc (1:1; P4C4-B10, gifted from B. A. Edgar, University of Washington, WA, USA), BrdU (1:500; BU-4, Takara) and Lamin (1:100; ADL84.12, DSHB). Secondary antibodies conjugated to Alexa 648 or 488 (Molecular Probes) were used at a dilution of 1:500. Cytosolic F-actin was stained with rhodamine-phalloidin (Molecular Probes). DNA was visualized with DAPI or 1 μM ToPro3 (Molecular Probes). For BrdU (5-bromo-2-deoxyuridine) labeling, dissected salivary glands were incubated in Schneider's medium (Gibco) containing 1 μg/ml BrdU for 45 minutes. Afterwards, they were fixed, washed, denatured in 2N HCl and neutralized in 100 mM sodium tetraborate. β-Gal activity was detected by incubating the discs in X-gal staining buffer. Images were photographed with a Carl Zeiss LSM710 laser scanning microscope.

Mitotic recombination

ssp mutant clones were generated by FLP/FRT-mediated somatic recombination. Clones were induced by heat shock at 37°C for 30 minutes. Larvae were dissected and fixed 48 hours after heat shock. The mutant clones can be recognized by the absence of GFP expression in the imaginal discs. Genotypes for generated clones are as follows: *y w hsp70-flp/y w dfz3^{J29}; ssp^{598} FRT3L2A/ub-GFPnls M(3)65F FRT3L2A*, *y w hsp70-flp; ssp^{598} FRT3L2A E2F-1-lacZ/ub-GFPnls M(3)65F FRT3L2A*, *y w hsp70-flp; PCNA-lacZ/+; ssp^{598} FRT3L2A/ub-GFPnls M(3)65F FRT3L2A*.

RT-PCR

For RT-PCR analysis of larvae, RNA was isolated from larvae using TRIsure (BIOLINE). Reverse transcription (RT) reactions were performed using 1 μg of total RNA and a poly-dT primer using Superscript reverse transcriptase III (Invitrogen). For PCR, the primer sequences used were as follows: *CG6801* [*l(3)j2D3* – FlyBase] forward primer, 5′-ATGCCGTCCAGAA-ATATTGACGATGCCG-3′; *CG6801* reverse primer, 5′-CTACTGATTG-TTATGCTTAAGCAAAT-3′; *ssp* (*CG1715* – FlyBase) forward primer, 5′-ATATCGAGCTGCTGCCCATCTCTAGGCAC-3′, *ssp* reverse primer, 5′-TGCATGTGCGCCGCCTTTGGGATTAGATAG-3′, *Actin 5C* (*Act5C* – FlyBase) forward primer; 5′-ATGTGTGACGAAGAAGTTGCTGCTC-TGGTT-3′, *Actin 5C* reverse primer; 5′-GAAGCACTTGCGGTGCACA-ATGGAGGGG-3′. *Actin 5C* was used as a control.

Quantitative RT-PCR

Ectopic expression was induced by a heat shock at 37°C for 30 minutes. Genotypes for heat-shocked larvae are as follows: *w; hs-Gal4/+; UAS-GFP/+*, *w; hs-Gal4/UAS-ssp*, *w; hs-Gal4/+; UAS-wg/+*. RT reactions were performed using 2 μg of total RNA and a random primer. For real-time PCR, the primer sequences used were as follows: *CG6801* forward primer, 5′-CGGAGTACGAGAAGTTCTACGAG-3′; *CG6801* reverse primer, 5′-GGCTTACGACGTTCTGGTGT-3′; *arm* forward primer, 5′-GTT-ACATGCCAGCCCAGAAT-3′; *arm* reverse primer, 5′-CTGCTCCTT-GGCGGATAC-3′; *E2F-1* (*E2f* – FlyBase) forward primer, 5′-TGG-AGCAACAGGAGAACGAG-3′; *E2F-1* reverse primer, 5′-GCGC-GGCAATTTTGTGT-3′; *PCNA* (*mus209* – FlyBase) forward primer, 5′-GGTCAAGCCACCATCCTGAA-3′; *PCNA* reverse primer, 5′-CAGC-GAGACAAGCGACACA-3′; *dfz3* (*fz3* – FlyBase) forward primer, 5′-GTCACACCAATCAGCTGGAG-3′; *dfz3* reverse primer, 5′-CGAGC-AGCCGGATTCTATTA-3′; *Actin 5C* forward primer, 5′-CCGACCGT-ATGCAGAAGGAG-3′; *Actin 5C* reverse primer, 5′-TGGAAGGTGGA-CAGCGAAG-3′.

Estimation of the relative nuclear area

The shape of the nuclear envelope visualized by staining with mAb against Lamin was regarded as an ellipse and its relative area was calculated by multiplying the lengths of the nuclear major and minor axes using Photoshop.

EMSA

^{32}P-labeled DNA probe (0.5 ng) was incubated with GST recombinant protein (1.5 μg) for 30 minutes in 20 μl of binding buffer [20 mM Tris-HCl (pH 8.0), 40 mM KCl, 6 mM MgCl$_2$, 1 mM EGTA, 1 mM DTT, 0.1% NP-40 and 10% glycerol]. The reaction mixture was loaded onto a gel containing 6% polyacrylamide and electrophoresed for 2 hours at 150 V. The gels were dried and quantified with a BAS1500 (Fujifilm) imaging analyzer. In competition assays, unlabeled competitor probe was added to the reaction mixture in a 5-fold molar excess relative to the radiolabeled probe. In Fig. 5C, GST recombinant protein was pre-incubated with anti-Ssp antibody or anti-FLAG antibody M2 (Sigma) for 12 hours at 4°C. SspΔBFD is a mutant lacking the BED finger domain (amino acids 34-98). The sequences of the probes used are shown in Fig. 5A.

RESULTS

Identification of Sunspot as an Armadillo-interacting protein

Arm is composed of 12 imperfect protein interaction repeats (Armadillo repeat domain) flanked by unique N and C termini (Fig. 1A). In an attempt to identify novel Arm-binding proteins, we performed a yeast two-hybrid screen of a *Drosophila* embryo cDNA library using the Armadillo repeat domain of Arm as bait (Fig. 1A). We isolated positive clones containing the same insert of a novel gene (*CG17153*) that we have named *sunspot* (*ssp*; named after the phenotype of mutant flies, see below). Sequence analysis of the full-length cDNA revealed that it encodes a protein of 368 amino acids. A region near its N terminus (amino acids 34
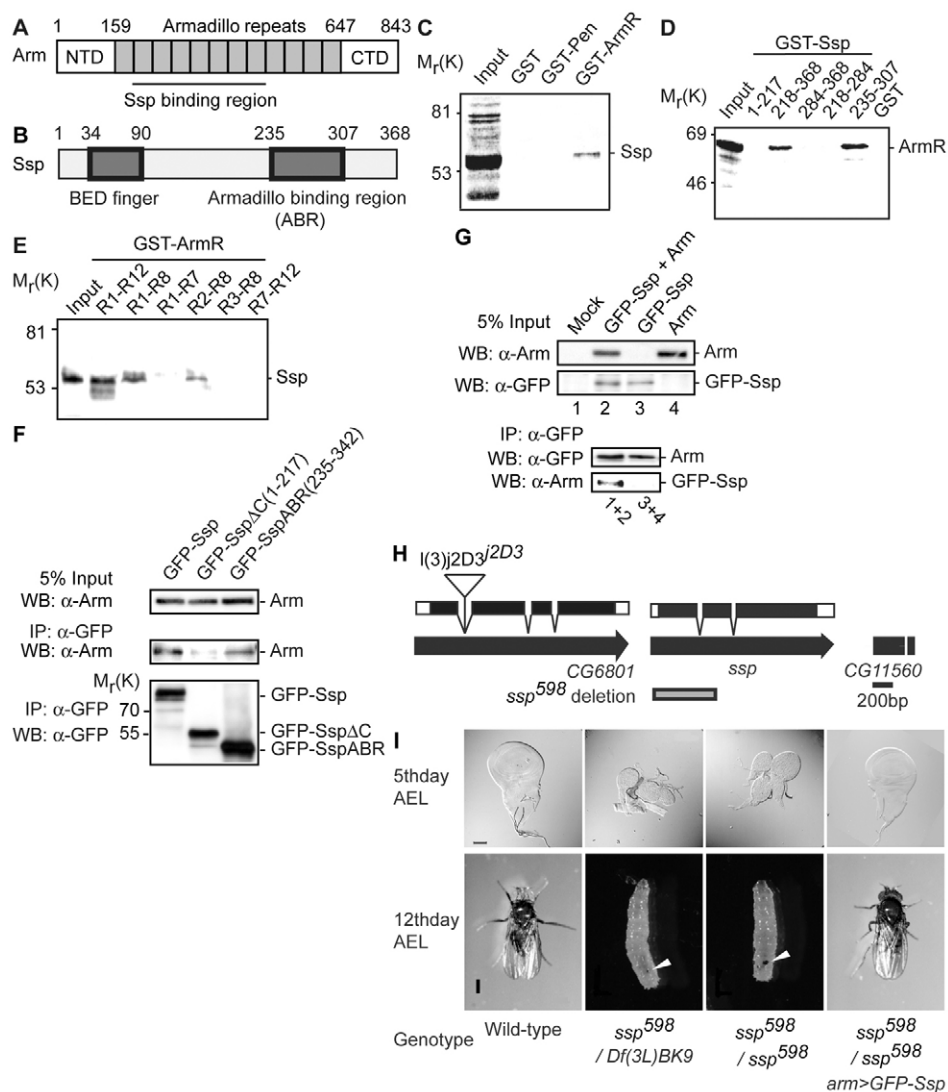
Fig. 1. Identification of Sunspot as an Armadillo-binding protein. (**A**) Schematic of the Arm protein. Arm consists of an N-terminal domain (NTD), a central region that spans 12 Armadillo repeats (labeled R1-R12) and a carboxy-terminal domain (CTD). Black bar indicates the experimentally determined binding site for Ssp. (**B**) Schematic of the Ssp protein. The BED finger motif and the Armadillo-binding region are highlighted in black. (**C**) Ssp binds to the Armadillo repeat domain of Arm. In vitro-translated Ssp was pulled down in the presence of GST, GST-Pen or GST-Armadillo repeat domain of Arm (GST-ArmR, amino acids 140-713). (**D**) Arm binds to amino acids 235 to 307 of Ssp. In vitro-translated ArmR was pulled down in the presence of GST or a series of deletion fragments of GST-Ssp. (**E**) Ssp binds to Armadillo repeats R2-R8. In vitro-translated Ssp was pulled down in the presence of a series of deletion fragments of GST-ArmR. (**F**) Ssp is associated with Arm in vivo. S2 cells were transfected with Arm and the indicated fragments of GFP-Ssp. Cell lysates were subjected to immunoprecipitation with GFP-TRAP-M followed by immunoblotting with anti-Arm antibody (middle panel) and anti-GFP-antibody (lower panel). Upper panel, inputs. (**G**) GFP-Ssp and Arm are associated in living cells. S2 cells were transfected with GFP-Ssp and/or Arm and subjected to immunoprecipitation with GFP-TRAP-M followed by immunoblotting with anti-Arm antibody (bottom). Upper panel, inputs. Lane 1, mock-transfected cells; lane 2, GFP-Ssp and Arm-coexpressing cells; lane 3, GFP-Ssp-expressing cells; lane 4, Arm-expressing cells. (Lower panel) 1+2, the lysates of mock-transfected cells and GFP-Ssp- and Arm-coexpressing cells were mixed and used for a pull-down assay; 3+4, the lysates of GFP-Ssp-expressing cells and Arm-expressing cells were mixed. (**H**) Structure of the *CG6801* and *ssp* transcripts. The triangle indicates the insertion site of the P-element *l(3)j2D3^{j2D3}*. Black and white boxes represent coding and non-coding sequences, respectively. Black arrows represent transcripts. Gray box represents sequences deleted in the *ssp^{598}* allele. Scale bar: 200 bp. (**I**) Microscope images of third instar imaginal discs at the fifth day after egg laying (AEL), and photographs of animals at the twelfth day AEL. Melanotic pseudotumors are indicated by arrowheads. Scale bars: 100 μm (fifth day AEL); 300 μm (twelfth day AEL).

to 98) shows similarity to the BED (BEAF and Dref) finger domain (Aravind, 2000), which is predicted to form a zinc finger and to bind DNA (Fig. 1B).

To confirm the interaction between Ssp and Arm, we examined whether Ssp produced by in vitro translation could interact with the Armadillo repeat domain of Arm fused to glutathione S-transferase

(GST). Ssp specifically interacted with the Armadillo repeat domain of Arm (amino acids 140 to 713), but failed to interact with Pendulin (Pen) (Kussel et al., 1995), a *Drosophila* homolog of importin α, which also possesses the Armadillo repeat domain (Fig. 1C; see also Fig. S1A in the supplementary material). Pull-down assays with a series of deletion fragments of Ssp showed that a fragment of Ssp
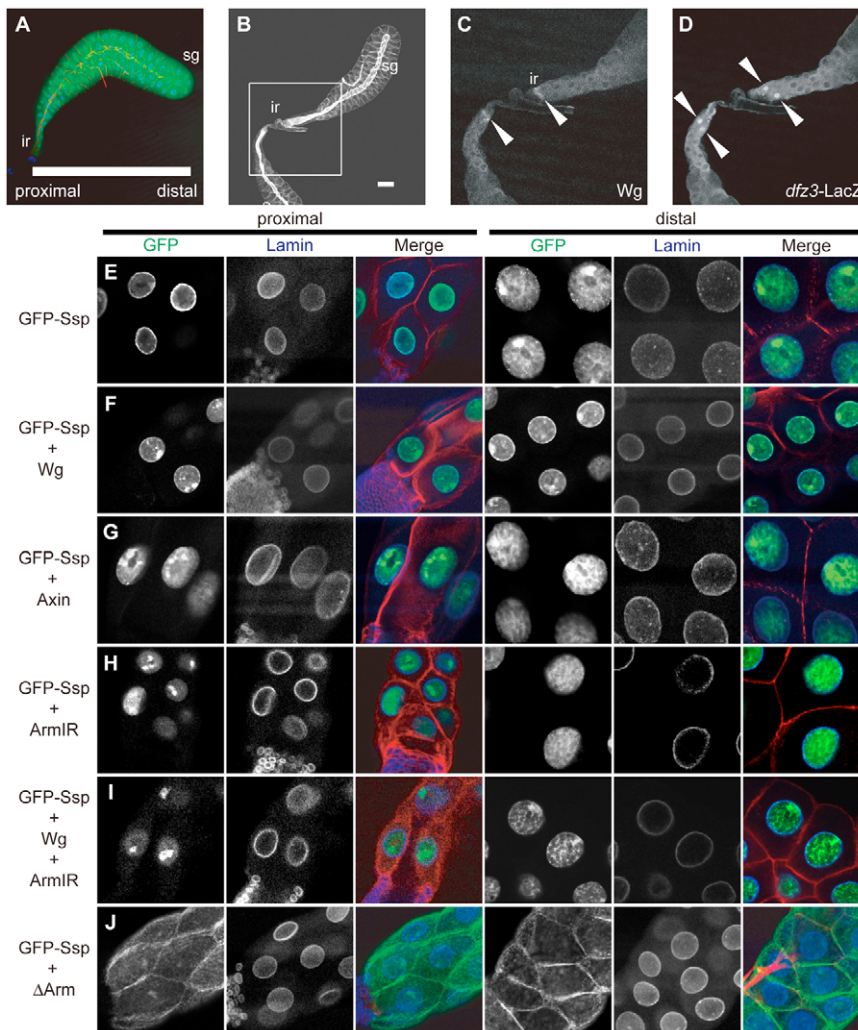
Fig. 2. Wg signaling regulates the subcellular distribution of GFP-Ssp in the third instar salivary gland. (**A**) *dpp-Gal4* expression visualized by *UAS-EGFP*. Glands were stained with rhodamine-phalloidin (red) and DNA was stained with ToPro3 (blue). (**B-D**) Salivary glands carrying *dfz3-lacZ* were stained with rhodamine-phalloidin (B), mAb against Wg (C) and β-gal (D). (C,D) The proximal region of the salivary gland outlined in white in B is shown at higher magnification. Arrowheads indicate Wg (C) and β-galactosidase (D) staining. (**E-J**) GFP-Ssp (green) was expressed in third instar salivary glands without (E) or with *UAS-Wg* (F), *UAS-Axin* (G), *UAS-ArmIR* (H,I) or *UAS-ΔArm* (membrane-targeted Arm; J). The effects of UAS-ArmIR on the expression of *Arm* and *dfz3* are shown in Fig. S3A in the supplementary material. Salivary glands were stained with rhodamine-phalloidin (red) and mAb against Lamin (blue). The proximal and distal regions of each gland are shown at higher magnification. ir, imaginal ring; sg, salivary gland. Scale bar: 100 μm.

containing amino acids 235 to 307 (termed the ABR, the Arm-binding region) binds to Arm in vitro (Fig. 1B,D; see also Fig. S1B in the supplementary material). Also, we found that Armadillo repeats 2-8 of Arm are responsible for binding to Ssp (Fig. 1A,E; see Fig. S1C in the supplementary material). Although TCF is known to bind to Armadillo repeats 3-10 of Arm (Graham et al., 2000; Poy et al., 2001), Ssp did not compete with TCF for binding to Arm (data not shown).

We next examined whether Ssp is associated with Arm in living cells. *Drosophila* Schneider-2 (S2) cells were transfected with Arm along with GFP-Ssp, GFP-SspΔC (amino acids 1 to 217; a mutant lacking the ABR) or GFP-SspABR (amino acids 235 to 342; a fragment containing the ABR). GFP-fusion proteins were immunoprecipitated from S2 cell lysates and subjected to immunoblotting with anti-GFP and anti-Arm antibodies. For immunoprecipitation of GFP-fusion proteins, we used a 13-kDa GFP-binding fragment derived from a llama single chain antibody, which was covalently immobilized to magnetic beads (GFP-Trap-M) (Rothbauer et al., 2008), as the molecular weight of GFP-SspΔC is the same as that of IgG. We found that Arm is associated with GFP-Ssp and GFP-SspABR (Fig. 1F). By contrast, Arm barely co-immunoprecipitated with GFP-SspΔC. In addition, we also performed pull-down assays with a mixture of lysates of S2 cells transfected with Arm alone and GFP-Ssp alone, respectively. We found that Ssp and Arm co-precipitate only when both proteins are

co-expressed in S2 cells, excluding the possibility that Ssp and Arm associate after cells are lysed (Fig. 1G). Taken together, these results suggest that Ssp interacts via its ABR with Arm not only in vitro but also in vivo.

Ssp is required for *Drosophila* development

We found one lethal *P*-element insertion line, $l(3)j2D3^{j2D3}$, in which a *P*-element had been inserted into the gene adjacent to *ssp*, *CG6801*, which is located about 250 bp upstream of the 5′ end of *ssp* (Fig. 1H). RT-PCR analysis revealed that the expression level and size of the CG6801 transcript were not changed compared with in wild-type larvae (see Fig. S2A in the supplementary material), which is consistent with the P-element being inserted into an intron in *CG6801*. To generate mutants that have a deletion in *ssp* but have intact *CG6801*, we used a local hop and imprecise excision approach (Preston et al., 1996). We used $l(3)j2D3^{j2D3}$ in a local hop to generate a *P*-element insertion line, $sunspot^P$, that completely complemented the lethality of $l(3)j2D3^{j2D3}$. We then generated *ssp* mutants by imprecise excision of the *P*-element from $sunspot^P$. We found one allele that has a deletion of about 600 bp and designated this as ssp^{598}. Sequence analysis showed that the deletion extends from a position 60 bp downstream of the presumptive *ssp* transcription start site to the *ssp* gene locus (Fig. 1G). Because this deletion removes the start codon and the BED finger domain of *ssp*, we presume that ssp^{598} represents a null allele for *ssp*. RT-PCR analysis revealed that ssp^{598}
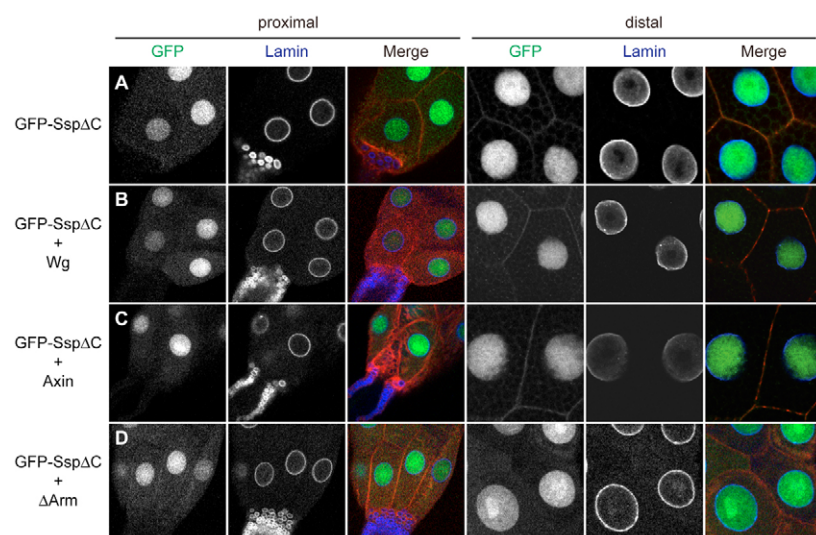
Fig. 3. Wg signaling does not regulate the subcellular distribution of GFP-SspΔC in the third instar salivary gland. (**A-D**) GFP-SspΔC (green) was expressed in third instar salivary glands without (A) or with *UAS-Wg* (B), UAS-Axin (C) or *UAS-ΔArm* (membrane-targeted Arm; D). Salivary glands were stained with rhodamine-phalloidin (red) and a mAb against Lamin (blue). Distal regions of each gland are shown at a higher magnification than the proximal regions.

generates a truncated transcript (see Fig. S2B in the supplementary material). The truncated transcript encodes a peptide consisting of 13 amino acids, which is unrelated to Ssp. By contrast, RT-PCR analysis revealed that the intact *CG6801* transcript is expressed in *ssp^598* mutant larvae, and that the expression level of *CG6801* is unchanged in *ssp^598* mutant larvae compared with that in wild-type larvae (see Fig. S2C,D in the supplementary material). Furthermore, *ssp^598* fully complemented the phenotype of *l(3)j2D3^j2D3* (data not shown), indicating that this mutant contains intact *CG6801*.

The imaginal discs, salivary glands and central nervous system of larvae homozygous for *ssp^598* were smaller than those of their normal counterparts (Fig. 1H; data not shown). *ssp^598* homozygotes reached the third instar stage, but failed to reach the pupal stage and died between 10 and 20 days after egg laying (AEL). Furthermore, melanotic pseudotumors were formed in *ssp^598* mutant larvae (Fig. 1H, arrowheads). Melanotic pseudotumors are groups of cells within the larvae that are recognized by the immune system and encapsulated within a melanized cuticle (Watson et al., 1991). One or more small melanotic pseudotumors first appeared in the *ssp* mutants at 6 days AEL, and the number and size of these melanotic pseudotumors increased during the development of the larvae. Similar phenotypes were observed with hemizygotes for *ssp*^598 and *Df(3L)BK9*, which has a deletion larger than that of *ssp^598* and lacks *ssp* (Fig. 1H). In situ hybridization analysis of imaginal discs using the coding region of the *ssp* cDNA as a probe revealed that *ssp* transcripts are expressed ubiquitously (see Fig. S2E-H in the supplementary material). We therefore examined whether ubiquitous expression of *ssp* restores the phenotypes of *ssp^598* homozygous animals. We found that ubiquitous expression of the full-length *ssp* cDNA with the Gal4-UAS system rescued the lethality and other phenotypes associated with *ssp^598* homozygous animals (Fig. 1H). Taken together, these results suggest that the phenotypes of *ssp^598* homozygotes are caused by the loss of *ssp* function, and that *ssp* is required for cell proliferation and morphogenesis of the imaginal disc and central nervous system.

Subcellular localization of Ssp is regulated by Wg signaling in the larval salivary gland

Arm is a key transducer of Wg signaling and many of the Arm-binding proteins are known to function as a component of the Wg signal transduction pathway (Riese et al., 1997; van de Wetering et al., 1997; Hamada et al., 1999a; Hamada et al., 1999b; Ahmed

et al., 2002; Kramps et al., 2002). To explore the possibility that Ssp is related to the Wg signal transduction pathway, we examined the effect of Wg on the distribution of GFP-Ssp. Because imaginal disc cells are too small for detailed study, we focused our analysis on the third instar salivary glands, and studied whether the subcellular localization of GFP-Ssp is linked to Wg signaling. The larval salivary gland mainly consists of secretory gland cells and imaginal ring cells (Fig. 2A,B). Gland cells are large polyploid epithelial cells. Small imaginal ring cells reside at the proximal end of the secretory gland. Immunostaining with anti-Wg antibody revealed that Wg is expressed in imaginal ring cells (Fig. 2C, arrowheads). Furthermore, *Drosophila frizzled 3 (dfz3)-lacZ*, a target gene of Wg signaling (Sato et al., 1999), was found to be expressed in imaginal ring cells and proximal gland cells, which reside within several cell diameters of the Wg-expressing cells (Fig. 2C,D, arrowheads) (see also Zecca et al., 1996; Neumann and Cohen, 1997; Tolwinski and Wieschaus, 2001). These results suggest that Wg signaling is active in the proximal region in the third instar salivary gland. When GFP-Ssp was expressed ubiquitously under the control of *dpp*-Gal4 (see Fig. 2A) in the larval salivary gland, GFP-Ssp was found to be localized predominantly at the nuclear envelope in proximal gland cells (Fig. 2E). In addition, GFP-Ssp was detected as aggregates in the nucleus in the distal region of the salivary gland (Fig. 2E). To examine whether this region-specific subcellular localization of GFP-Ssp is related to Wg signaling, we overexpressed Wg or Axin, a negative regulator of Wg signaling, in the salivary gland under the control of *dpp*-Gal4 (Hamada et al., 1999b; Tolwinski and Wieschaus, 2001). We found that expression of Wg along with GFP-Ssp resulted in the accumulation of a certain population of GFP-Ssp at the nuclear envelope in both the distal and proximal regions (Fig. 2F). Again, a significant amount of GFP-Ssp was localized in nuclear aggregates in both distal and proximal cells, suggesting that ectopic expression of Wg can also change the subnuclear localization of Ssp in proximal cells, from the nuclear periphery to nuclear aggregates. This result also suggests that ectopic expression of Wg in distal cells is not sufficient to change the subnuclear localization of all GFP-Ssp protein, from nuclear foci to the nuclear periphery. By contrast, when Axin was expressed along with GFP-Ssp, GFP-Ssp was detected as nuclear aggregates, not only in the distal region but also in the proximal region (Fig. 2G), but was no longer detected at the nuclear
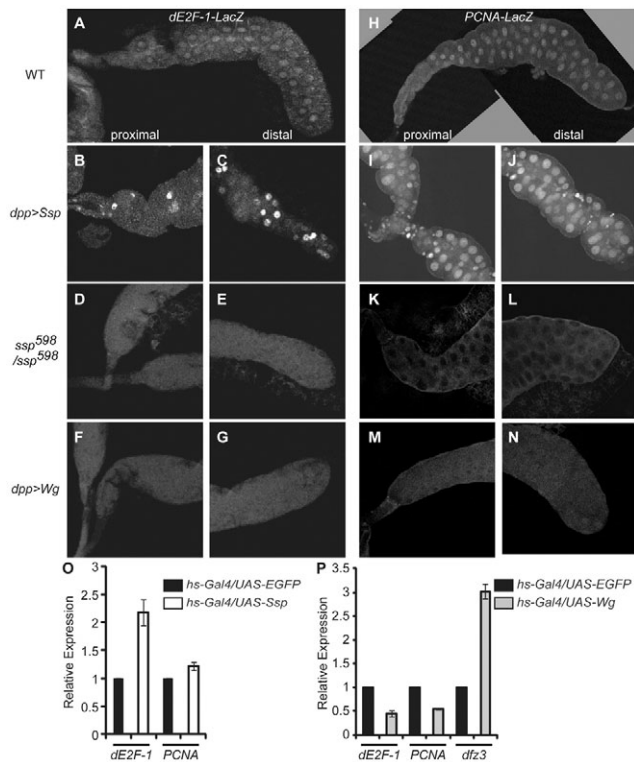
Fig. 4. Ssp positively regulates *dE2F-1* and *PCNA* expression in the third instar salivary gland. (A-N) Salivary glands from third instar larvae with various genotypes were stained with mAbs against β-gal. (B,D,F,I,K,M) Proximal region; (C,E,G,J,L,N) distal region. Genotypes are as follows: (A) *dpp-Gal4, dE2F-1-lacZ/+,* (B,C) *UAS-Ssp/+; dpp-Gal4, dE2F-1-lacZ/+,* (D,E) *dE2F-1-lacZ, ssp598/ssp598,* (F,G) *dpp-Gal4, dE2F-1-lacZ/UAS-Wg,* (H) *PCNA-lacZ/+; dpp-Gal4/+,* (I,J) *PCNA-lacZ/UAS-Ssp; dpp-Gal4/+,* (K,L) *PCNA-lacZ/+; ssp598/ssp598,* (M,N) *PCNA-lacZ/+; dpp-Gal4/UAS-Wg.* (O,P) Quantitative RT-PCR analysis of the *dE2F-1, PCNA* and *dfz3* transcripts from whole third instar larvae after heat shock, using *hs-Gal4* to drive the indicated transgenes. *dfz3* was used as a positive control of a Wg target gene. The *y-*axis shows relative expression of *UAS-Ssp* (O) or *UAS-Wg* (P) relative to *UAS-EGFP.* Prior to fold change calculation, values were normalized by *Actin 5C* mRNA. Results are expressed as the mean ± s.e.m.

envelope. These results suggest that the subcellular localization of Ssp is regulated at least in part by Wg signaling in the third instar salivary gland.

To examine whether the effect of Wg signaling on Ssp localization is mediated by the direct interaction between Arm and Ssp, we studied Ssp localization in larvae expressing an RNAi targeting Arm. We found that Ssp was localized in nuclear aggregates and that Wg overexpression did not alter its localization when the expression of Arm was suppressed by RNAi (Fig. 2H,I; see Fig. S3A in the supplementary material). Thus, Arm is required for Wg-induced Ssp relocalization. We also examined Ssp localization in cells expressing ΔArm, a mutant of Arm that localizes at the plasma membrane (Zecca et al., 1996; Tolwinski and Wieschaus, 2001). We found that overexpression of ΔArm under the control of *dpp*-Gal4 results in the localization of GFP-Ssp at the plasma membrane throughout the salivary gland (Fig. 2J; see also Fig. S3B in the supplementary material). We next examined the subcellular localization of SspΔC, a mutant that lacks the ABR and
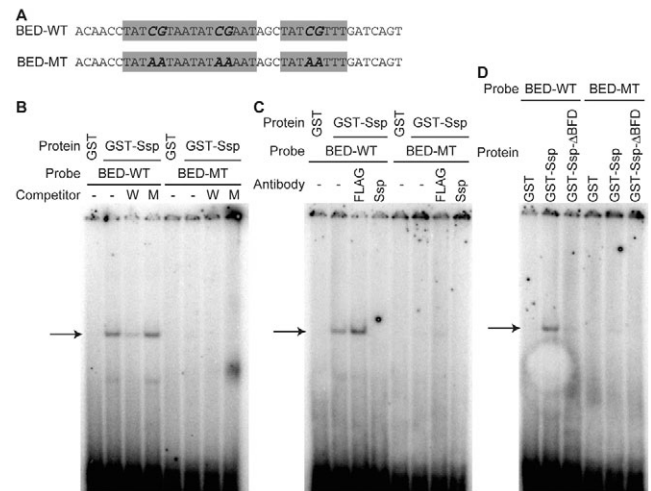

Fig. 5. Ssp binds to BBEs in the *dE2F-1* promoter. (A) Sequences of DNA probes BED-WT and -MT. Probe BED-WT contains three BBEs (encompassed in gray boxes). In probe BED-MT, GC in each BBE is replaced with AA (bold letters). (B) Ssp binds to BBEs. ^{32}P-labeled probe BED-WT or -MT was incubated with GST or GST-Ssp as indicated. DNA-protein interactions were analyzed by EMSA. Unlabeled probe BED-WT or -MT was used as a competitor. (C) Anti-Ssp antibody inhibits the interaction between Ssp and BBEs. ^{32}P-labeled probe BED-WT or -MT was incubated with GST or GST-Ssp that had been pre-incubated in the presence or absence of anti-Ssp antibody as indicated. Anti-FLAG antibody was used as a negative control. (D) Ssp binds to BBEs via its BED finger domain. ^{32}P-labeled probe BED-WT or -MT was incubated with GST, GST-Ssp or GST-SspΔBFD as indicated.

is unable to interact with Arm (see Fig. 1B,F). When GFP-SspΔC was expressed ubiquitously, it was found to localize homogenously in the nucleus of both distal and proximal cells (Fig. 3A). This result indicates that the localization of Ssp to nuclear aggregates requires the ABR and suggests that Ssp requires a direct interaction with Arm to localize to its target sites in the nucleus. Furthermore, we found that the localization of GFP-SspΔC was not changed by coexpression with Wg (Fig. 3B), Axin (Fig. 3C), or ΔArm (Fig. 3D). Taken together, these results suggest that the direct interaction between Arm and Ssp is required for the regulation of Ssp localization by Wg signaling.

Ssp controls transcription of genes involved in cell proliferation

The N-terminal region of Ssp contains a BED finger domain (see Fig. 1B). This presumptive DNA-binding domain is known to be contained in several *Drosophila* proteins, such as Dref and BEAF-32 (Hirose et al., 1993; Hirose et al., 1996; Zhao et al., 1995). Dref regulates the transcription of genes involved in DNA replication and cell proliferation, including *dE2F-1 and PCNA,* the promoters of which contain BED finger-binding elements (BBEs) (Sawado et al., 1998; Hochheimer et al., 2002). To clarify whether Ssp regulates the transcription of these genes, we examined the expression levels of *dE2F-1* and *PCNA.* For this purpose, we used the P-element (*lacZ*) insertion lines *E2F*[07172] (Duronio and O'Farrell, 1995) and *PCNA*[02248] (Pflumm and Botcha, 2001). *dE2F-1-lacZ* and *PCNA-lacZ* expression were found to be high in distal cells compared with proximal cells in the larval salivary gland (Fig. 4A,H). When *ssp* was ectopically expressed in the salivary gland, *dE2F-1-lacZ*
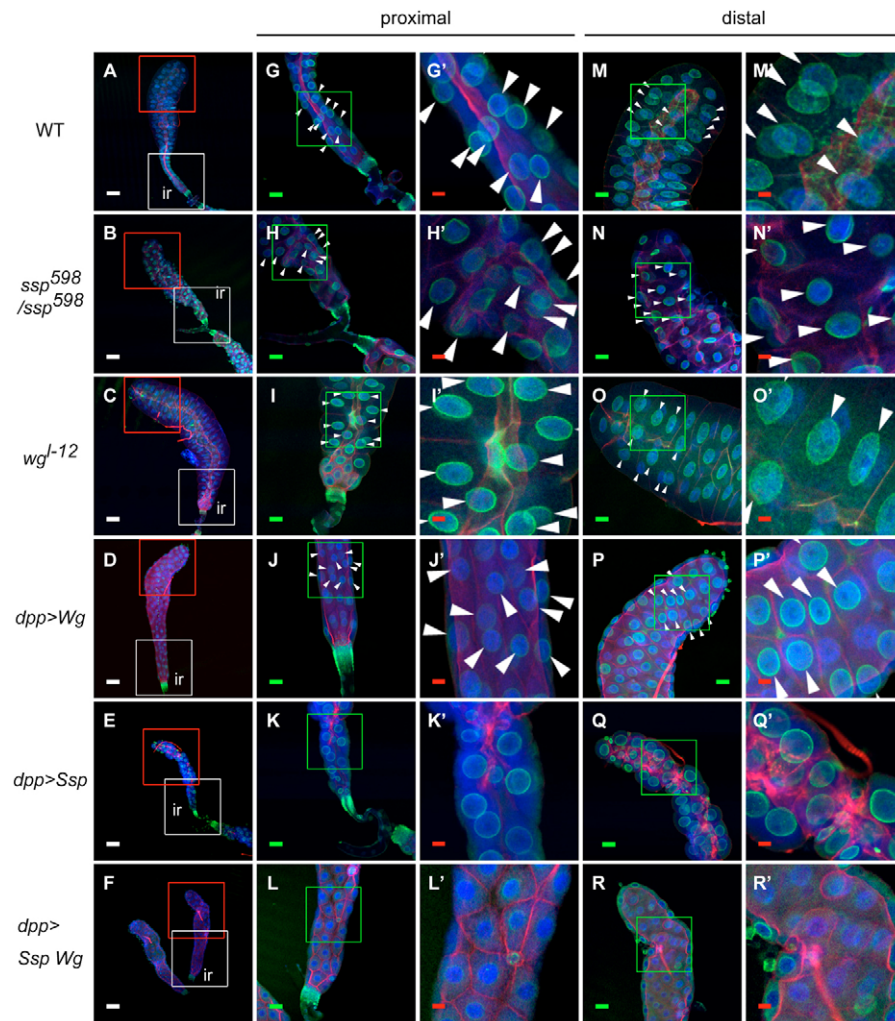
Fig. 6. Graded ploidy needs cooperation between Ssp and Wg in the third instar salivary gland. (**A-R**) Salivary glands from third instar larvae with various genotypes were stained with mAb against Lamin (green) and phalloidin (red). DNA was stained with ToPro3 (blue). (G-L) Magnification of the proximal regions outlined in white in A-F. (G'-L') Magnification of the regions outlined in green in G-L. (M-R) Magnification of the distal regions outlined in red in A-F. (M'-R') Magnification of the regions outlined in green in M-R. (A,G,G',M,M') Wild-type salivary gland. (B,H,H',N,N') ssp^{598} homozygous salivary gland. (C,I,I',O,O') wg^{I-12} homozygous salivary gland. Salivary glands overexpressing Wg (D,J,J',P,P'), Ssp (E,K,K',Q,Q'), Wg and Ssp (F,L,L',R,R') are also shown. ir, imaginal ring. Scale bars: white, 100 μm; green, 33 μm; red, 11 μm.

expression was markedly elevated in distal cells, whereas it was only slightly elevated in proximal cells (Fig. 4B,C). However, *PCNA-lacZ* expression was markedly elevated throughout the salivary gland (Fig. 4I,J). By contrast, *dE2F-1-lacZ* and *PCNA-lacZ* expression were not elevated in distal cells of *ssp* mutant salivary glands compared with in wild-type salivary glands (Fig. 4D,E,K,L), and *dfz3-lacZ* expression in ssp mutant and Ssp-overexpressing salivary glands was not changed compared with in wild-type salivary glands (Fig. 2B-D; see also Fig. S4A-D in the supplementary material), suggesting that Ssp is not involved in Arm-dTCF-mediated transactivation of Wg target genes. In addition, overexpression of Wg resulted in a decrease in the expression levels of *dE2F-1-lacZ* and *PCNA-lacZ* in distal cells (Fig. 4F,G,M,N). Thus, Ssp is active in the distal region where Wg signaling is not active, and Ssp is aggregated in the nucleus. Conversely, Ssp is not very active in the proximal region where Wg signaling is active, and Ssp is accumulated in the nuclear envelope.

We also examined the expression of *dE2F-1*, *PCNA* and *dfz3* in the wing disc. We generated clones of cells lacking Ssp function by FLP/FRT-mediated somatic recombination. Clones of *ssp* mutant cells underwent only a few divisions after they were generated in the presumptive wing blade (data not shown): the mutant cells proliferated slowly and either died or were actively eliminated from the disc epithelium. Therefore, we used a *Minute* mutation, *M(3)65F*, to confer a growth advantage upon cells homozygous for

ssp. When mitotic recombination was induced in a *M(3)65F* background using enhancer trap lines, *ssp* mutant cells exhibited reduced levels of *dE2F-1-lacZ* and *PCNA-lacZ* expression but did not show any change in the levels of *dfz3-lacZ* and Arm expression (see Fig. S5A-G in the supplementary material). These results suggest that *ssp* regulates the expression of *dE2F-1* and *PCNA*, but is not involved in Arm-dTCF-mediated Wg signaling.

To confirm these results, we examined endogenous expression of *dE2F-1* and *PCNA* by quantitative real-time RT-PCR analysis using RNA from late third instar larvae. Flies carrying heat-shock-inducible Gal4 (*hs*-Gal4) were crossed with transgenic flies carrying *UAS-GFP*, *UAS-ssp* or *UAS-wg*. Consistent with the above results, overexpression of *ssp* resulted in elevated steady state levels of *dE2F-1* and *PCNA* transcripts (Fig. 4O). Furthermore, overexpression of Wg induced decreases in the numbers of *dE2F-1* and *PCNA* transcripts (Fig. 4P). These results suggest that *dE2F-1* and *PCNA* expression is regulated positively by Ssp and negatively by Wg.

We also examined whether Ssp regulates the expression of *dE2F-1* by binding directly to its promoter region. Electrophoretic mobility-shift assays (EMSA) showed that GST-Ssp, but not GST, bound to a 40-mer oligonucleotide corresponding to a region in the *dE2F-1* promoter that contains three BBEs (Fig. 5A,B; see also Fig. S1D in the supplementary material). By contrast, GST-Ssp barely bound to a mutated probe in which CG in each BBE
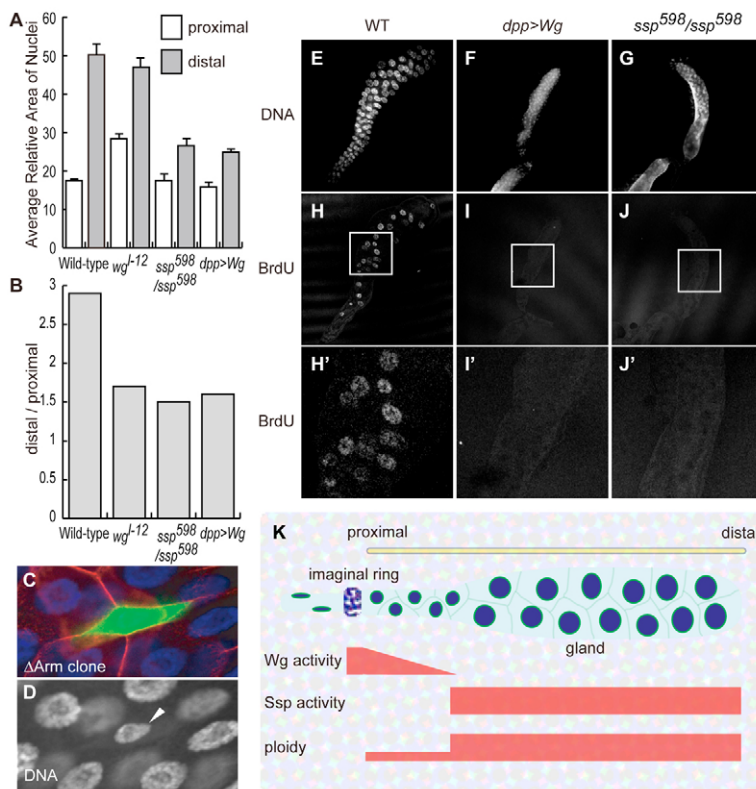
Fig. 7. Graded ploidy needs cooperation between Ssp and Wg in the third instar salivary gland. (**A**) Graphical representation of the average relative areas of the nuclei that are indicated by arrowheads in Fig. 6G-J,M-P. White and gray bars represent the average relative nuclear areas in the proximal and distal regions, respectively. Results are expressed as the mean ± s.e.m. (**B**) Graphical representation of the ratio of the average relative nuclear areas of the distal cells to those of the proximal cells. (**C,D**) A ΔArm (activated form of Armadillo)-expressing clone (*Act>Gal4;UAS-GFP UAS-ΔArm*) in the salivary gland. The ΔArm-expressing clone was labeled by coexpression of GFP (green); the glands were stained with rhodamine-phalloidin (red); DNA (D) was stained with ToPro3 (blue). (D) The arrowhead indicates the nucleus of the ΔArm-expressing cell. (**E-J**) Salivary glands from wild-type and mutant third instar larvae were dissected and incubated in the presence of BrdU. Salivary glands were stained with a mAb against BrdU (H-J) and DNA (E-G) was visualized with ToPro3. (**H′-J′**) Magnification of the salivary glands outlined in white in H-J. Genotypes are as follows: (E,H,H′) wild type; (F,I,I′) *dpp-Gal4;UAS-Wg*; (G,J,J′) *ssp598/ssp598*. (**K**) Ssp and Wg regulate endoreplication in the salivary gland. The Wg signal represses the function of Ssp by altering the subcellular localization of Ssp, and thereby negatively regulates the endoreplication of proximal cells.

had been replaced with AA. Binding of Ssp to the wild-type probe was inhibited in the presence of an excess amount of unlabeled wild-type probe, whereas the mutated probe did not inhibit the interaction significantly. When anti-Ssp antibody was included in the reaction mixture, the Ssp band was not detected (Fig. 5C). Furthermore, we found that GST-SspΔBFD, a mutant Ssp lacking the BED finger domain, did not bind to the wild-type probe (Fig. 5D; see also Fig. S1D in the supplementary material). These results suggest that Ssp regulates *dE2F-1* expression by binding directly to the BBEs in the *dE2F-1* promoter region via its BED finger domain.

Ssp and Wg regulate endoreplication in the third instar salivary gland

To further elucidate the function of Ssp and Wg, we examined the third instar salivary glands of *ssp* and *wg* mutants (Bejsovec and Martinez Arias, 1991). In the third instar salivary gland, the distal region undergoes greater endoreplication than does the proximal region (Pierce et al., 2004; Edgar and Orr-Weaver, 2001). As a result, the nuclear size of distal gland cells is markedly larger than that of proximal gland cells (Fig. 6A,G,G′,M,M′; Fig. 7A). However, the nuclear size of *ssp* mutant distal cells was found to be smaller than that of wild-type distal cells (Fig. 6B,H,H′,N,N′; Fig. 7A,B). By contrast, the nuclear size of *wg* mutant proximal cells was larger than that of wild-type proximal cells (Fig. 6C,I,I′,O,O′; Fig. 7A). Thus, the difference in nuclear size between proximal and distal cells was also small in the salivary glands of *wg* mutants (Fig. 7B).

To confirm these results, we examined the effects of Ssp and/or Wg overexpression on the nuclear size of salivary gland cells. When Ssp was overexpressed, the nuclear size of both proximal and distal cells was heterogenous (Fig. 6E,K,K′,Q,Q′). Overexpression of Wg decreased the nuclear size of distal cells (Fig. 6D,J,J′,P,P′): the

difference in nuclear size between Wg-overexpressing proximal and distal cells was small (Fig. 7B). However, when Wg was overexpressed along with Ssp, the effect of Ssp was suppressed and the heterogeneity of nuclear size was not observed (Fig. 6F,L,L′,R,R′). Furthermore, to confirm that Ssp and Wg play important roles in the regulation of endoreplication, we generated ΔArm-expressing clones using the flip-out technique. We found that the nuclear size of ΔArm-expressing cells is much smaller than that of surrounding cells (Fig. 7C,D, arrowhead). This result suggests that ΔArm mislocalizes Ssp to the plasma membrane, thereby negatively regulating Ssp activity for endoreplication.

To directly show that *ssp* mutant cells undergo fewer endoreplications than do wild-type cells, we performed BrdU-labeling experiments. When wild-type salivary glands were labeled with BrdU, distal cells efficiently incorporated BrdU (Fig. 7E,H,H′), indicating that they underwent at least one round of DNA replication during the labeling period. By contrast, very few nuclei of *ssp* mutant cells and Wg-overexpressing cells were labeled with BrdU (Fig. 7F,G,I-J′).

dMyc (Dm – FlyBase) has also been reported to be required for the endoreplication of salivary gland cells (Pierce et al., 2004). It is therefore interesting to examine the relationship between dMyc, Wg and Ssp in endoreplication. We found that dMyc expression was unchanged in both *ssp* mutant and Ssp-overexpressing salivary glands (see Fig. S6A-H in the supplementary material). Thus, Ssp might not be involved in the regulation of dMyc.

Taken together, these results suggest that Ssp and Wg play important roles in the regulation of endoreplication in the third instar salivary gland, and that Wg might exert its effect by negatively regulating the function of Ssp (Fig. 7K). It is interesting to speculate that Ssp plays a general role for endoreplication in all larval endocycling tissues.

DISCUSSION

It is believed that Wg/Wnt target genes are transactivated by Arm/β-catenin associated with TCF (Moon et al., 2004; Clevers, 2006). However, expression of some human genes is transactivated by β-catenin that is associated with proteins other than TCF. For example, β-catenin interacts with the androgen receptor in an androgen-dependent manner and enhances androgen-mediated transactivation (Terry et al., 2006). In the present study, we have shown that Arm interacts with Ssp and negatively regulates its function. Ssp transactivates *dE2F-1* and *PCNA* expression, and positively regulates the endoreplication of salivary gland cells. Furthermore, the Wg signal represses the function of Ssp by altering the subcellular localization of Ssp in the salivary gland: the Wg signal induces the accumulation of Ssp at the nuclear envelope (Fig. 2E-J; Fig. 6; Fig. 7). Interestingly, recent studies indicate that the nuclear membrane provides a platform for sequestering transcription factors away from their target genes. For example, it has been shown that the tethering of transcription factors such as c-Fos and R-Smads to the nuclear envelope prevents transcription of their target genes (Heessen and Fornerod, 2007). Our results appear to be consistent with these findings. Although the precise mechanism remains to be investigated, the interaction between Arm and Ssp appears to be required for the regulation of Ssp localization by Wg signaling. It remains to be investigated whether the mechanisms identified in the salivary gland are applicable to other tissues.

Competing interests statement

The authors declare no competing financial interests.

Supplementary material

Supplementary material for this article is available at
http://dev.biologists.org/lookup/suppl/doi:10.1242/dev.042077/-/DC1

References

Ahmed, Y., Nouri, A. and Wieschaus, E. (2002). Drosophila Apc1 and Apc2 regulate Wingless transduction throughout development. *Development* **129**, 1751-1762.

Aravind, L. (2000). The BED finger, a novel DNA-binding domain in chromatin-boundary-element-binding proteins and transposases. *Trends Biochem. Sci.* **25**, 421-423.

Bejsovec, A. and Martinez Arias, A. (1991). Roles of wingless in patterning the larval epidermis of Drosophila. *Development* **113**, 471-485.

Bienz, M. (2002). The subcellular destinations of APC proteins. *Nat. Rev. Mol. Cell Biol.* **3**, 328-338.

Cadigan, K. M. and Nusse, R. (1997). Wnt signalling: a common theme in animal development. *Genes Dev.* **11**, 3286-3305.

Clevers, H. (2006). Wnt/beta-catenin signaling in development and disease. *Cell* **127**, 469-480.

Duronio, R. J. and O'Farrell, P. H. (1995). Developmental control of the G1 to S transition in Drosophila: cyclin Eis a limiting downstream target of E2F. *Genes Dev.* **9**, 1456-1468.

Edgar, B. A. and Orr-Weaver, T. L. (2001). Endoreplication cell cycles: more for less. *Cell* **105**, 297-306.

Fodde, R., Smits, R. and Clevers, H. (2001). APC signal transduction and genetic instability in colorectal cancer. *Nat. Rev. Cancer* **1**, 55-67.

Graham, T. A., Weaver, C., Mao, F., Kimmelman, D. and Xu, W. (2000). Crystal structure of a -catenin/Tcf complex. *Cell* **103**, 885-896.

Greaves, S., Sanson, B., White, P. and Vincent, J. P. (1999). A screen for identifying genes interacting with armadillo, the Drosophila homolog of beta-catenin. *Genetics* **153**, 1753-1766.

Guder, C., Philipp, I., Lengfeld, T., Watanabe, H., Hobmayer, B. and Holstein, T. W. (2006). The Wnt code: cnidarians signal the way. *Oncogene* **25**, 7450-7460.

Hamada, F., Murata, Y., Nishida, A., Fujita, F., Tomoyasu, Y., Nakamura, M., Toyoshima, K., Tabata, T., Ueno, N. and Akiyama, T. (1999a). Identification and characterization of E-APC, a novel Drosophila homologue of the tumour suppressor APC. *Genes Cells* **4**, 465-474.

Hamada, F., Tomoyasu, Y., Takatsu, Y., Nakamura, M., Nagai, S., Suzuki, A., Fujita, F., Shibuya, H., Toyoshima, K., Ueno, N. et al. (1999b). Negative regulation of Wingless signaling by D-axin, a Drosophila homolog of axin. *Science* **283**, 1739-1742.

He, T. C., Sparks, A. B., Rago, C., Hermeking, H., Zawel, L., da, Costa, L. T., Morin, P. J., Vogelstein, B. and Kinzler, K. W. (1998). Identification of c-MYC as a target of the APC pathway. *Science* **281**, 1509-1512.

Heessen, S. and Fornerod, M. (2007). The inner nuclear envelope as a transcription factor resting place. *EMBO Rep.* **8**, 914-919.

Hirose, F., Yamaguchi, M., Handa, H., Inomata, Y. and Matsukage, A. (1993). Novel 8-base pair sequence (Drosophila DNA replication-related element) and specific binding factor involved in the expression of Drosophila genes for DNA polymerase alpha and proliferating cell nuclear antigen. *J. Biol. Chem.* **268**, 2092-2099.

Hirose, F., Yamaguchi, M., Kuroda, K., Omori, A., Hachiya, T., Ikeda, M., Nishimoto, Y. and Matsukage, A. (1996). Isolation and characterization of cDNA for DREF, a promoter-activating factor for Drosophila DNA replication-related genes. *J. Biol. Chem.* **271**, 3930-3937.

Hochheimer, A., Zhou, S., Zheng, S., Holmes, M. C. and Tjian, R. (2002). TRF2 associates with DREF and directs promoter-selective gene expression in Drosophila. *Nature* **420**, 439-445.

Kinzler, K. W. and Vogelstein, B. (1996). Lessons from hereditary colorectal cancer. *Cell* **87**, 159-170.

Kramps, T., Peter, O., Brunner, E., Nellen, D., Froesch, B., Chatterjee, S., Murone, M., Zullig, S. and Basler, K. (2002). Wnt/wingless signaling requires BCL9/legless-mediated recruitment of pygopus to the nuclear beta-catenin-TCF complex. *Cell* **109**, 47-60.

Kussel, P. and Frasch, M. (1995). Pendulin, a Drosophila protein with cell cycle-dependent nuclear localization, is required for normal cell proliferation. *J. Cell Biol.* **129**, 1491-1507.

Moon, R. T., Kohn, A. D., De Ferrari, G. V. and Kaykas, A. (2004). WNT and beta-catenin signaling: diseases and therapies. *Nat. Rev. Genet.* **5**, 691-701.

Morin, P. J., Sparks, A. B., Korinek, V., Barker, N., Clevers, H., Vogelstein, B. and Kinzler, K. W. (1997). Activation of beta-catenin-Tcf signaling in colon cancer by mutations in beta-catenin or APC. *Science* **275**, 1787-1790.

Nagase, H. and Nakamura, Y. (1993). Mutations of the APC (adenomatous polyposis coli) gene. *Hum. Mutat.* **2**, 425-434.

Neumann, C. J. and Cohen, S. M. (1997). Long-range action of Wingless organizes the dorsal-ventral axis of the Drosophila wing. *Development* **124**, 871-880.

Peifer, M. and Polakis, P. (2000). Wnt signalling in oncogenesis and embryogenesis-a look outside the nucleus. Science **287**, 1606-1609.

Pflumm, M. F. and Botchan, M. R. (2001). Orc mutants arrest in metaphase with abnormally condensed chromosomes. *Development* **128**, 1697-1707.

Pierce, S. B., Yost, C., Britton, J. S., Loo, L. W., Flynn, E. M., Edgar, B. A. and Eisenman, R. N. (2004). dMyc is required for larval growth and endoreplication in Drosophila. *Development* **131**, 2317-2327.

Preston, C. R., Sved, J. A. and Engels, W. R. (1996). Flanking duplications and deletions associated with P-induced male recombination in Drosophila. *Genetics* **144**, 1623-1638.

Price, M. A. (2006). CKI, there's more than one: casein kinase I family members in Wnt and Hedgehog signaling. *Genes Dev.* **20**, 399-410.

Poy, F., Lepourcelet, M., Shivdasani, R. A. and Eck, M. J. (2001). Structure of a human Tcf4-beta-catenin complex. *Nat. Struct. Biol.* **8**, 1053-1057.

Riese, J., Yu, X., Munnerlyn, A., Eresh, S., Hsu, S. C., Grosschedl, R. and Bienz, M. (1997). LEF-1, a nuclear factor coordinating signaling inputs from wingless and decapentaplegic. *Cell* **88**, 777-787.

Rothbauer, U., Zolghadr, K., Muyldermans, S., Schepers, A., Cardoso, M. C. and Leonhardt, H. (2008). A versatile nanotrap for biochemical and functional studies with fluorescent fusion protein. *Mol. Cell Proteomics* **7**, 282-289.

Rubinfeld, B., Robbins, P., El-Gamil, M., Albert, I., Porfiri, E. and Polakis, P. (1997). Stabilization of beta-catenin by genetic defects in melanoma cell lines. *Science* **275**, 1790-1792.

Sato, A., Kojima, T., Ui-Tei, K., Miyata, Y. and Saigo, K. (1999). Dfrizzled-3, a new Drosophila Wnt receptor, acting as an attenuator of Wingless signaling in wingless hypomorphic mutants. *Development* **126**, 4421-4430.

Sawado, T., Hirose, F., Takahashi, Y., Sasaki, T., Shinomiya, T., Sakaguchi, K., Matsukage, A. and Yamaguchi, M. (1998). The DNA replication-related element (DRE)/DRE-binding factor system is a transcriptional regulator of the Drosophila E2F gene. *J. Biol. Chem.* **273**, 26042-26051.

Segditsas, S. and Tomlinson, I. (2006). Colorectal cancer and genetic alterations in the Wnt pathway. *Oncogene* **25**, 7531-7537.

Terry, S., Yang, X., Chen, M. W., Vacherot, F. and Buttyan, R. (2006). Multifaceted interaction between the androgen and Wnt signaling pathways and the implication for prostate cancer. *J. Cell Biochem.* **99**, 402-410.

Tolwinski, N. S. and Wieschaus, E. (2001). Armadillo nuclear import is regulated by cytoplasmic anchor Axin and nuclear anchor dTCF/Pan. *Development* **128**, 2107-2117.

van de Wetering, M., Cavallo, R., Dooijes, D., van Beest, M., van Es, J., Loureiro, J., Ypma, A., Hursh, D., Jones, T. Bejsovec, A. et al. (1997). Armadillo coactivates transcription driven by the product of the Drosophila segment polarity gene dTCF. *Cell* **88**, 789-799.

Watson, K. L., Johnson, T. K. and Denell, R. E. (1991). Lethal(1) aberrant immune response mutations leading to melanotic tumor formation in Drosophila melanogaster. *Dev. Genet.* **12**, 173-187.

Yan, D., Wiesmann, M., Rohan, M., Chan, V., Jefferson, A. B., Guo, L., Sakamoto, D., Caothien, R. H., Fuller, J. H. and Reinhard, C. et al. (2001). Elevated expression of axin2 and hnkd mRNA provides evidence that Wnt/beta -catenin signaling is activated in human colon tumors. *Proc. Natl. Acad. Sci. USA* **98**, 14973-14978.

Zecca, M., Basler, K. and Struhl, G. (1996). Direct and long-range action of a wingless morphogen gradient. *Cell* **87**, 833-844.

Zhao, K., Hart, C. M. and Laemmli, U. K. (1995). Visualization of chromosomal domains with boundary element-associated factor BEAF-32. *Cell* **81**, 879-889.